

High-Arsenic Groundwater from Huaihe River Basin, China—Geochemistry and Hydrogeochemical Processes

Naizheng Xu (✉ xzzz100@sina.com)

China Geological Survey Nanjing Center

Jianshi Gong

China Geological Survey Nanjing Center

Yonghong Ye

China Geological Survey Nanjing Center

Research Article

Keywords: arsenic (As), groundwater pollution, hydrogeochemistry, water-rock interaction, Huaihe River Basin

Posted Date: June 30th, 2021

DOI: <https://doi.org/10.21203/rs.3.rs-605688/v1>

License:   This work is licensed under a Creative Commons Attribution 4.0 International License.

[Read Full License](#)

Abstract

Arsenic (As) poses a danger to environmental health, and drinking arsenic-rich groundwater is a key exposure risk for humans. The distribution, migration, and enrichment of As in groundwater is an important worldwide environmental and public health problem that requires research. Huaihe River Basin has been newly identified as a region of high-arsenic groundwater in China. This study aims to analyze the hydrogeochemical data of high-arsenic groundwater, trace its formation and evolution, and evaluate its potential pollution risks. The results showed that As and F were the main inorganic chemical substances affecting the water quality in the study area, with concentrations of $5.75\pm 5.42 \mu\text{g L}^{-1}$ and $1.29\pm 0.40 \text{ mg L}^{-1}$, respectively, exceeding the recommended drinking water standards of the World Health Organization by 23% and 31%, respectively. The proportion of groundwater with a high As content presents a high exposure risk. According to the hydrochemical diagram and the calculation of mineral saturation indices, the groundwater in the study area underwent evaporation, halite dissolution, and water-rock interaction. The total alkalinity of high-arsenic groundwater ranges mainly between 400–700 mg L^{-1} , and the chemical type is mainly of $\text{HCO}_3\text{-Na}$. High-arsenic groundwater is largely affected by evaporation and cation exchange. In an alkaline environment, As in high-arsenic groundwater derives from the dissolution and release of arsenic sulfide in aquifer sediments and poses a potential threat to human health through food and drinking water.

1. Introduction

Arsenic (As) is ubiquitous in nature and listed as a Class-I specific carcinogen by the International Agency for Research on Cancer (IARC) (Shahid et al., 2018; WHO, 2011). The most sensitive toxicity threshold of As concentration in drinking water has not been determined. The recommended limit of As concentration in drinking water is $10 \mu\text{g L}^{-1}$ according to the guidelines for drinking-water quality by the World Health Organization (WHO, 2011). According to the United States Environmental Protection Agency (EPA) and the National Research Council (NRC), the long-term consumption of water with As concentrations as low as $5 \mu\text{g/L}$, or even $3 \mu\text{g/L}$, may cause adverse chronic health effects on humans, especially cancer (Taheri et al., 2017). Drinking groundwater rich in As is the main route for human exposure to this element. Globally, more than 100 million people are exposed to high-arsenic groundwater, including 19 million in China (Cao et al., 2018; Duan et al., 2017; Li et al., 2017; Shahid et al., 2018).

The formation of high-arsenic groundwater is a result of the combined action of multiple factors and complex geological processes. Many researchers have conducted in-depth and extensive geochemical studies on the distribution areas of high-arsenic groundwater. They have analyzed its formation and evolution and traced the source of arsenic and its dissolution and release mechanisms (Gan et al., 2014; Gao et al., 2020a,b; Fan et al., 2017; Hu et al., 2015; Kumar et al., 2017; Li et al., 2013; Li et al., 2018; Tang et al., 1996; Wang et al., 1998; Zhang et al., 2017). Huaihe River Basin is an area in China where high-arsenic groundwater has been newly discovered. Ever since arsenic in drinking-water was discovered in this basin in the 1980s, the enrichment of arsenic in groundwater in this area has received extensive

attention, and preliminary hydrogeological environmental surveys and scientific research have been conducted (Chen et al., 2013; Li et al., 2017; Wen et al., 2013; Zhang et al., 2010). A statistical prediction based on groundwater data from Huaihe River Basin was conducted in 2010. The analysis found that the probability of arsenic exposure risk in Huaihe River Basin was predicted to be greater than 0.40 and the proportion of As concentration exceeding $10 \mu\text{g}\cdot\text{L}^{-1}$ in the monitored wells of villages in the statistical survey area was 17%, with the highest detection value being $620 \mu\text{g}\cdot\text{L}^{-1}$ (Li et al., 2017). Previous research has mainly focused on the hydrogeochemical distribution of high-arsenic groundwater and the geographical distribution of endemic diseases as a consequence water arsenic poisoning through drinking water. Such research has lacked in-depth analyses of the formation processes, evolution mechanisms, and influencing factors that result in high-arsenic groundwater.

There are many aquifers in Huaihe River Basin. Due to the long-term and large-scale exploitation of groundwater, the environment of the groundwater flow system has changed, potentially leading to the reduction or oxidative dissolution of arsenic minerals in the aquifer, and posing a potential threat to human health through, for example, food and drinking water. Given the extensive harmful effects of arsenic on the natural environment and public health, conducting geochemical studies on arsenic pollution in groundwater of Huaihe River Basin is necessary. This study selected the representative small-scale flow field of high-arsenic groundwater in the Huaihe River Plain (Taihe County, Anhui Province) to analyze the sources and occurrence of arsenic contaminants and identify the hydrogeochemical processes. This may provide a scientific basis and engineering reference for the treatment and public health risk control of arsenic contamination.

2. Study Area

Huaihe River Basin is located in Eastern China. It originates in Tongbai and Funiu Mountains in the west, faces the Yellow Sea in the east. The geographical coordinates are $111^{\circ}55'E$ to $121^{\circ}25'E$ and $30^{\circ}55'N$ to $36^{\circ}36'N$, with an area of 270,000 km^2 . Huaihe River Basin is located in the north and south climatic transition zone in China and belongs to the warm temperate subhumid monsoon climate zone, with an annual average temperature of $11-16^{\circ}\text{C}$. Huaihe River Basin is geologically located at the junction of three tectonic units that are the North China Block, the Yangtze Block and the Qinling Orogenic Belt (Zhang et al., 2015). The terrain tilts slightly from northwest to southeast, with alluvial-proluvial plain as the main landform. The terrain is flat, with sea-level elevation generally ranging from 15 to 50 meters (Fig. 1).

Since the Neogene period (23 Ma), loose Neogene and Quaternary sediments of immense thickness have formed in Huaihe River Basin, providing good hydrogeological conditions for the formation and distribution of groundwater in the region. The groundwater system of Huaihe River Basin is divided into shallow, middle and deep aquifer systems, from top to bottom, and groundwater flow runs from northwest to Southeast generally. The shallow groundwater occurs in the Holocene and late Pleistocene strata of 50 m and is influenced by meteoric precipitation and surface water. The groundwater depth is generally 2–4 m within the limit of evaporation depth, and evaporation is the main drainage route of

shallow groundwater. The middle groundwater occurs in the middle and lower Pleistocene strata of 50–150 m, while the deep groundwater mainly occurs in the Neogene strata of 150–500 m (Fig. 1). Due to the deep burial of the middle and deep groundwater (buried depth of more than 50 m), the aquifers that are separated by cohesive soil layers cannot directly receive the recharge from atmospheric precipitation and the runoff is slow. Exploitation is the main method through which deep groundwater gets discharged.

3. Methods

According to the principle of thermodynamics, the dissolution and precipitation of minerals in water-rock reactions are determined by the saturation index (SI) of various minerals in groundwater. The SI can be used to identify the water quality and hydrochemical evolution process (Han et al., 2014; Taheri et al., 2017; Zhu et al., 2011).

The mathematical expression of SI is:

$$SI = \lg IAP/K_s$$

where IAP is the ionic active product and K_s is the equilibrium constant of the mineral.

$SI < 0$, $SI = 0$ and $SI > 0$ are the thermodynamic criteria for the dissolution, equilibrium, and precipitation of minerals, respectively, and $0.5 > SI > -0.5$ is generally considered as near saturation.

According to the analysis of a hydrogeological survey recently conducted in Huaihe River Basin, Taihe County in Anhui Province is a typical high-arsenic groundwater area in the Huaihe River Plain (Fig. 1). For this study, we selected a small-scale zone of high-arsenic groundwater in Maji Town as a natural experimental field to collect and test groundwater samples. The groundwater sampling points were selected via the grid method, with an accuracy of 1 km × 0.5 km or 1 km × 1 km, and 62 water samples were collected. All the groundwater samples were from the shallow aquifer, which formed during the Holocene to Late Pleistocene, with 4–50 m deep water tables. The aquifers consist of quaternary sandstone, fine sandstone, and siltstone. An instantaneous sampling method was implemented for groundwater sample collection. Before sampling, sample bottles and stopcocks were washed three to five times with the water to be collected; then, the samples were acidified with nitric acid ($\text{pH} < 2$) for the analysis of cations. The pH, temperature and total dissolved solids (TDS) were measured in the field using portable meters (HANNA, HI8424; **THERMO scientific, ORION**) and calibrated using standard solution.

All samples collected and analyzed in this study were from shallow pore groundwater and the porous water system formed during the Holocene to Late Pleistocene. The hydrochemical concentrations of ions such as As, K^+ , Na^+ , Ca^{2+} , Mg^{2+} , Cl^- , SO_4^{2-} , HCO_3^- , F^- , and Br^- , total alkalinity, and total acidity were determined at the Laboratory of the China Geological Survey Nanjing Center. The As concentration in the groundwater was determined by atomic fluorescence spectrometry. The detection limit of As by fluorescence spectrometer (AFS-820, China) was $0.05 \mu\text{g}\cdot\text{L}^{-1}$, with $< 1.0\%$ precision. Cations (Na^+ , K^+ , Ca^{2+} ,

Mg²⁺) were determined by inductively coupled plasma-atomic emission spectrometry (ICP-OES), while anions (SO₄²⁻, Cl⁻, F⁻, Br⁻) were determined via ion chromatography. Total alkalinity and total acidity, and HCO₃⁻ were determined by acid titration. There were 42 in-situ sediment samples collected for X-ray diffraction, determined by X-ray diffractometer (D/MAX 2500, Japan) at the Laboratory of the China Geological Survey Nanjing Center.

For the statistical analysis, SPSS19.0 was used as a platform for the descriptive statistical analysis, correlation analysis, and regression analysis. Phreeqc 3.40 was selected for determination the mineral phase and saturation indices. The thematic maps were produced by using Coreldraw X4 and AquaChem 3.70.

4 Results And Discussion

4.1 Major ions and hydrochemistry

Fig. 1 shows the results of sampling and analysis in May and September 2019. According to the results of the hydrochemical analysis, the TDS concentration of the shallow groundwater was 719±310 mg L⁻¹. Most of the samples were low-salinity fresh water (< 1000 mg L⁻¹) and 26% were in the range of brackish water (1000–3000 mg L⁻¹). The mean annual temperature of the groundwater samples is approximately 17.1°C, with a range of from 16.6°C–17.3°C. The average pH value is 7.31, with a range of from 7.01–8.19, which shows little variation across the study area. The chemical composition of groundwater was mainly controlled by ions (SO₄²⁻, Cl⁻, HCO₃⁻, Na⁺, Ca²⁺, Mg²⁺). The anion components were mainly HCO₃⁻, followed by SO₄²⁻ and Cl⁻, with concentrations of 617±220, 83.7±73.1, and 54.0±58.8 mg L⁻¹, respectively. The dominant cation was Na⁺, followed by Ca²⁺ and Mg²⁺, with concentrations of 186±120, 46.2±27.9, and 39.5±12.4 mg L⁻¹, respectively. According to the drinking water quality standards recommended by the WHO (2011), the main factors affecting the groundwater quality in the study area were the concentrations of As and F. The As concentration of groundwater in the study area was 5.75±5.42 µg L⁻¹, showing clear spatial variability. The proportion of high-arsenic groundwater samples above 1 µg L⁻¹ reached 74%, nearly 1/4 of which exceeded the threshold of > 10 µg L⁻¹ recommended by the WHO (Fig. 1). The F⁻ concentration of groundwater was 1.29±0.40 mg L⁻¹, and 31% of the considered samples exceeded the WHO-recommended limit of 1.50 mg L⁻¹.

The dominant ions determine the groundwater types. According to the Piper diagram (Fig. 2), the groundwater types in the study area are dominated by HCO₃⁻Na, followed by HCO₃⁻Na·Mg, HCO₃⁻Na·Ca, and HCO₃⁻Na·Ca·Mg. The high-arsenic groundwater types are dominated by HCO₃⁻Na (Fig. 2).

4.2 Hydrogeochemical processes

4.2.1 Evaporation and dissolution processes Water-rock interaction is a critical process in determining the chemical composition of groundwater. Hydrogeochemical processes such as dissolution, ion exchange,

oxidation, and reduction occurring in the process of water-rock interaction are the main factors controlling the chemical characteristics of groundwater. The hydrogeochemical processes were identified based on distinct hydrochemicals and their concentrations (Gibbs, 1970; Liu et al., 2018; Taheri et al., 2017; Xing et al., 2013; Zhu et al., 2011). The Gibbs diagram is an analytical method that uses the relationship between the ratios of $\text{Na}/(\text{Na} + \text{Ca})$ and $\text{Cl}/(\text{Cl} + \text{HCO}_3)$, and TDS to reflect the controlling factors of main ions in the water. According to the Gibbs diagram (Fig. 3), TDS in the study area was $722 \pm 296 \text{ mg L}^{-1}$, $\text{Cl}/(\text{Cl} + \text{HCO}_3)$ ranged from 0.01 to 0.03, and $\text{Na}/(\text{Na} + \text{Ca})$ ranged from 0.23 to 0.94. Most of the analytical samples were located in the areas of water-rock interaction and evaporation crystallization (Fig. 3), confirming that the water-rock interaction and evaporation processes have an impact on the formation and evolution of groundwater in the study area.

In this study, PHREEQC 3.40 was used to calculate the mineral saturation indices, indicating that the SI values of near-saturated minerals, calcite (0.41), aragonite (0.26), and magnesite (0.04), were close to 0 and in a quasi-equilibrium state. The SI values of the unsaturated minerals, halite (-6.52), gypsum (-1.99), anhydrite (-2.23), and fluorite (-1.018), were less than -0.5, indicating a dissolution tendency. The SI of dolomite (0.70) was greater than 0.5, indicating a chemical precipitation tendency (Table 1). Cl^- , F^- and SO_4^{2-} in groundwater were partly derived from the dissolution and release of halite, fluorite, gypsum, and anhydrite minerals.

Table 1. Saturation indices in groundwater from Taihe, Anhui Province, in Huaihe River Basin, China

Sample grouping ID	SI(h)	SI(g)	SI(an)	SI(d)	SI(c)	SI(ar)	SI(f)	SI(m)
Group 1: $\text{As} \leq 3 \mu\text{g L}^{-1}$;	-6.80	-1.94	-2.18	1.02	0.47	0.32	-0.87	0
Group 2: $5 \leq \text{As} < 10 \mu\text{g L}^{-1}$;	-6.32	-1.94	-2.19	0.50	0.42	0.27	-1.02	0.12
Group 3: $10 \leq \text{As} < 50 \mu\text{g L}^{-1}$;	-6.43	-2.06	-2.31	0.94	0.36	0.21	-1.12	0.02
Group 4: $\text{As} \geq 50 \mu\text{g L}^{-1}$	-6.52	-2.00	-2.25	0.35	0.38	0.23	-1.06	0.02

SI(h): halite, SI(g): gypsum, SI(d): dolomite, SI(c): calcite,

SI(f): Fluorite, SI(an): anhydrite, SI(m): Magnesite, SI(ar): Aragonite

4.2.2 Evaporation and concentration processes—Solutes also commonly found in groundwater are Cl and Br. Due to the conservative behavior and high solubility of Cl and Br in natural water, ion exchange reaction and mineral surface adsorption cannot significantly change the concentrations of Cl and Br. With the increase of chloride ion concentration, the dissolution of halite (NaCl) will produce a rapid increase in the Cl/Br ratio. In contrast, the evaporation process of groundwater can change the absolute concentrations of Cl and Br in groundwater, but will not change the Cl/Br ratio before the groundwater is saturated with halite. Therefore, Cl, Br, and Cl/Br ratios can be used to identify and distinguish the dissolution, evaporation, and other evolution processes of groundwater (Cartwright et al., 2006; Deng et

al., 2009; Han et al., 2014; Taheri et al., 2017; Xie et al., 2012; Xing et al., 2013). The Cl^- concentration range of the test samples was $0.70\text{--}210 \text{ mg L}^{-1}$, the mean value was $54.0 \pm 58.8 \text{ mg L}^{-1}$, the Br^- concentration range was $10.7\text{--}324 \text{ } \mu\text{g L}^{-1}$, and the mean value was $104 \pm 88 \text{ } \mu\text{g L}^{-1}$. There was a significant positive correlation between the Cl^- and Br^- concentrations, with a correlation coefficient of 0.75 ($P \leq 0.01$). As the Cl^- and Br^- concentrations of the test samples were relatively low, the mean value of Cl^-/Br^- (mol) was 1097 ± 1044 and the ratio varied from 51.0 to 4603. A majority of Cl^-/Br^- ratios of the test samples exceeded 600, showing significant spatial variability. The Cl^-/Br^- ratios of water samples above the WHO limit ($\geq 10 \text{ } \mu\text{g L}^{-1}$) ranged from 544 to 3093, with an average of 993. The mineral structure of halite (NaCl) does not contain large Br^- , and its Cl^-/Br^- ratios are generally $10^4\text{--}10^5$. The dissolution of halite will result in the rapid increase of Cl^-/Br^- ratio with the increase of Cl^- concentration. The highest value of Cl^-/Br^- ratios of the test samples exceeded 4600, and the concentration of Cl^- in groundwater did not exceed 6 mmol L^{-1} . The dissolution of a small amount of halite in groundwater was the most likely mechanism for the rapid increase of Cl^-/Br^- ratios. The large variation range of Cl^-/Br^- ratios reflected the different dissolved amount of halite in each test sample. As shown by the relationship between Cl^-/Br^- ratios and Cl^- concentrations (Fig. 4), evaporation and halite dissolution are the dominant processes controlling the distribution of shallow groundwater. The Cl^-/Br^- ratios of high-arsenic groundwater are relatively unchanged with the increase of Cl^- concentrations, indicating that the high-arsenic groundwater is more affected by evaporation.

4.2.3 Ion exchange processes The Na^+/Cl^- ratio (mol) is a hydrogeochemical parameter characterizing the degree of Na^+ enrichment in groundwater that can be used to reflect the degree of ion exchange (Han et al., 2014; Taheri et al., 2017; Xing et al., 2013; Yang et al., 2016). Huaihe River Basin is an arid- semi-arid region with strong evaporation, which leads to the accumulation of halite in the sedimentary layer. The dissolution of halite is one of the sources of Na^+ and Cl^- in groundwater in basin regions. If the dissolution of halite is the main source of Na^+ and Cl^- , the ratio of Na^+/Cl^- (mol) should be 1:1, and Na^+ above this ratio may have other sources. In this study, the Na^+/Cl^- ratios of groundwater samples collected in the entire region were 9.63 ± 57.4 and those of most samples were substantially larger than 1:1, showing significant spatial variability. The Na^+/Cl^- ratio decreased with the increase of Cl^- concentration. The Na^+/Cl^- ratios of contaminated groundwater ($\text{As} \geq 10 \text{ } \mu\text{g L}^{-1}$) were 15.7 ± 16.0 , above the dissolution line of halite (Fig. 5). It can therefore be inferred that the Na^+ of groundwater in the study area is not derived only from the dissolution of halite. The groundwater may experience overall strong cation exchange and the ion exchange of high-arsenic groundwater is more significant.

4.4 Source of arsenic and its mobilization

Under the pH and Eh conditions of the natural environment, arsenic exists mainly as $\text{As}(\text{V})$ in an inorganic oxidation state or $\text{As}(\text{III})$ in a reduction state. Arsenic minerals in sediments usually exist in mineral phases such as arsenate, arsenite, and sulfide. There are many possible hydrogeochemical factors that trigger the release of arsenic from the solid phase into the groundwater. Changes in groundwater regime, redox potential (Eh), acidity, and alkalinity (pH) exert an influence on arsenic in sediments, through the

adsorption and resolution process and then affect the concentration of As in water (Chen et al, 2017; Wang et al., 2015; Duan et al., 2017; Gao et al., 2020b; Gao et al., 2010; Elizabeth et al., 2019; Huang et al., 2012; Taheri et al., 2017; Zhang et al., 2017).

Alkalinity is a chemical measurement of a water's ability to neutralize acids. Alkalinity is also a measure of a water's buffering capacity or its ability to resist changes in pH upon the addition of acids or bases (Rice et al., 2012). The alkalinity in natural water mainly depends on the presence of bicarbonate (HCO_3^-), carbonate (CO_3^{2-}) and hydroxide (OH^-). The total alkalinity of the test samples was $515 \pm 169 \text{ mg L}^{-1}$, the total acidity was $20.0 \pm 4.63 \text{ mg L}^{-1}$, and the groundwater was alkaline. According to the law of carbonate balance, when the pH value is 4.5–10, the HCO_3^- alkalinity occurs. When the pH value is ≤ 8.32 , all CO_3^{2-} is converted to HCO_3^- (Chen et al., 2009; Yang et al., 2016; Zhu et al., 2011). The total alkalinity of the test samples had a highly significant positive correlation with the concentration of HCO_3^- , with a correlation coefficient $R=0.997$ ($P \leq 0.01$). Therefore, the total alkalinity in the water samples is HCO_3^- alkalinity and it generally reflects the content of HCO_3^- . The total alkalinity of high-arsenic groundwater was mainly ranged between $400\text{--}700 \text{ mg L}^{-1}$. The weathering of carbonate mineral and ion exchange reactions in the study area increased the alkalinity of the groundwater.

The SO_4^{2-} in the groundwater could be derived from both gypsum dissolution and sulfide oxidation and there was a positive correlation between As and SO_4^{2-} contents in the test samples (correlation coefficient $R=0.58$) (Fig. 6). The mean concentrations of SO_4^{2-} in the groundwater with $\text{As} < 3$, $3 \leq \text{As} < 5$, $5 \leq \text{As} < 10$ and $\text{As} \geq 10 \text{ } \mu\text{g L}^{-1}$ in the analytical samples were 0.74, 1.09, 0.92, and 0.93 mmol L^{-1} , respectively, and the high-arsenic groundwater showed a relatively high SO_4^{2-} concentration. The $\text{SO}_4^{2-}/\text{Ca}^{2+}$ (mol) ratio of groundwater in the entire region was 0.76. SO_4^{2-} in the groundwater originated not only from the dissolution of gypsum minerals, but also from the oxidation of sulfide.

According to the phase analysis by X-ray diffraction, the main mineral components of the sediments in Huaihe River Basin are quartz, potash feldspar, calcite and clay minerals, with the contents of 47.1%, 3.79%, 8.27% and 33.4%, respectively. There are a small amount of pyrite and siderite in some samples, the contents are 2.5% and 47.1% respectively. No hematite is detected. Under reduction conditions, Arsenic sulfide is a stable host of arsenic, and its associated arsenic is highly correlated with the occurrence of groundwater arsenic (Duan et al., 2017; Elizabeth et al., 2019; Hu et al., 2015; Shahid et al., 2018; Taheri et al., 2017; Zhang et al., 2017). Therefore, it is speculated that arsenic in sediments from Huaihe River Basin may exist as arsenic-bearing sulfides phase under reduction conditions.

Due to the long-term exploitation of groundwater in large quantities, the environment of the groundwater flow system has changed, breaking the equilibrium of dynamic exchange between the solid and liquid phases of the aquifers, and triggering the release of arsenic from the solid phase into the groundwater. The dissolution of carbonate minerals usually increases the alkalinity (pH). Under high pH conditions, the oxidation of arsenic-containing sulfide leads to the release of arsenic and sulfur into the groundwater,

promoting concentration of arsenic and SO_4^{2-} . The increase in pH also promotes the desorption of arsenic from iron manganese oxides, thereby increasing the concentration of As in groundwater (Duan et al., 2017; Elizabeth et al., 2019; Taheri et al., 2017; Zhang et al., 2017).

5. Conclusion

The formation of high-arsenic groundwater requires the combined action of multiple factors in the process of water-rock interaction, such as the accumulation of arsenic-bearing minerals, the dissolution and precipitation of solid arsenic, and the hydrogeological conditions of arsenic enrichment. Huaihe River Basin is a typical area of high-arsenic groundwater in China. In this study, we selected a typical small-scale region of high-arsenic groundwater in the basin for the natural field experiment to analyze the formation and evolution of high-arsenic groundwater and trace the source of arsenic and its release mechanism. The concentration of As in groundwater in the study area was $5.75 \pm 5.42 \mu\text{g L}^{-1}$, showing clear spatial variability. The proportion of groundwater with a high As content ($\geq 1 \mu\text{g L}^{-1}$) reached 74%, showing a high exposure risk. According to the analysis of hydrochemical composition, the groundwater in the study area underwent the effects of evaporation, halite dissolution, and water-rock interaction. Cl^- , F^- and SO_4^{2-} in the groundwater are partly derived from the dissolution and release of halite, fluorite, gypsum, and anhydrite minerals. The chemical type of high-arsenic groundwater is mainly $\text{HCO}_3\text{-Na}$. High-arsenic groundwater is affected significantly by evaporation and cation exchange. The high-arsenic groundwater is of in-situ origin, and arsenic probably derived from the dissolution and release of the primary arsenic in the aquifer sediments. In an alkaline environment, the oxidative dissolution of arsenic-containing sulfide is the main process leading to the formation of high-arsenic groundwater.

Declarations

Acknowledgements

This research was financially supported by the Science and Technology Programme of the Jiangsu Province (SBK2020022002, SBE2020740286) and the Chinese Project of the National Geological Survey (DD20190354).

References

1. Cartwright I, Weaver T, Fifield L (2006) Cl/Br ratios and environmental isotopes as indicators of recharge variability and groundwater flow: An example from the southeast Murray Basin, Australia. *Chemical Geology* 231: 38–56.
2. Cao HL, Xie XJ, Wang YX, Pi KF, Li JX, Zhan HB, Liu P (2018) Predicting the risk of groundwater arsenic contamination in drinking water wells. *Journal of Hydrology* 560:318–325.

3. Chen J, Qian H, Wu H, Gao YY, Li XY (2017) Assessment of arsenic and fluoride pollution in groundwater in Dawukou area, Northwest China, and the associated health risk for inhabitants. *Environ Earth Sci* 76:314.
4. Chen Y, Sun YJ, Wang FF, Wang YN, Lu M, Zhang DL (2013) Research on arsenic contents and its speciation distribution in sediments of northern suburb water source field in Zhengzhou. *Journal of Qingdao Technological University* 34 (5): 55-60.
5. Chen ZJ, Zhu J, Zhang J (2009) The properties of groundwater chemical composition by gray relevancy analysis in Boertala, Xinjiang. *Journal of Salt Lake Research* 17(1):27-30.
6. Deng YM, Wang YX, Ma T (2009) Isotope and minor element geochemistry of high arsenic groundwater from Hangjinhouqi, the Hetao Plain, Inner Mongolia. *Applied Geochemistry* 24: 587-599.
7. Duan YH, Gan YC, Wang YX (2017) Arsenic speciation in aquifer sediment under varying groundwater regime and redox conditions at Jiangnan Plain of Central China. *Science of the Total Environment* 607–608: 992–1000.
8. Elizabeth CG, Audrey RM, Owen WD, Rebecca BN, Matthew LP (2019) Chemical variability of sediment and groundwater in a Pleistocene aquifer of Cambodia: Implications for arsenic pollution potential. *Geochimica et Cosmochimica Acta* 245: 441–458.
9. Gan YC, Wang YX, Duan YH (2014) Hydrogeochemistry and arsenic contamination of groundwater in the Jiangnan Plain, central China. *Journal of Geochemical Exploration* 138. 81–93.
10. Gao CR, Liu WB, Liu B (2010) Modes of occurrence of arsenic in Quaternary sediments of the Hetao Plain. *Geology In China* 37(3):760-770.
11. Gao YY, Qian H, Huo CC, Chen J, Wang HK (2020a) Assessing natural background levels in shallow groundwater in a large semiarid drainage Basin. *Journal of Hydrology* 584:124638.
12. Gao YY, Qian H, Wang HK, Chen J, Ren W.H, Yang FX (2020b) Assessment of background levels and pollution sources for arsenic and fluoride in the phreatic and confined groundwater of Xi'an city, Shaanxi, China. *Environmental Science and Pollution Research* 27:34702–34714.
13. Garbinski LD, Rosen BP, Chen J (2019) Pathways of arsenic uptake and efflux. *Environment International* 126:585–597.
14. Gupta PK, Joshi P, Jahangeer (2017) In-situ observation and transport modelling of arsenic in Gangetic plain, India. *Emerging Contaminants* 3: 138-143
15. Han DM, Song XF, Currell MJ, Yang JL, Xiao GQ (2014) Chemical and isotopic constraints on evolution of groundwater salinization in the coastal plain aquifer of Laizhou Bay, China. *Journal of Hydrology* 508: 12–27.
16. Gan Y, Zhang JM, Zhang YF, Zhang X (2017) Distribution regularity origin and quality division of high arsenic, fluorine and iodine contents in groundwater in Datong basin. *Geological survey of China* 4(1):57-68.
17. Hu YH, Zhou L, Li X, Xu FD, Wang L, Mo DZ, Zhou L, Wang X (2015) Arsenic contamination in Shimen Realgar mine As spatial distribution, chemical fractionations and leaching. *Journal of Agro-Environment Sciences* 34(8): 1515-1521

18. Li B, Zhao CJ, Li PY, Yuan Y (2013) BCR speciation analysis of arsenic in contaminated soil in arsenic mining area. *Journal of Yunnan University for Nationalities: Natural Science* 22(5):330-333.
19. Li MY, Liu YG, Hou L, Zheng Y, Qi DH, Zhao R, Ren W (2018) Effects and concentration prediction of environmental factors on the speciation of arsenic in the sediments of Yangzonghai lakeside wetland. *Research of Environmental Sciences* 31 (9): 1554-1563.
20. Li YF, Wang D, Liu YY, Zheng QM, Sun GF (2017) A predictive risk model of groundwater arsenic contamination in China applied to the Huai River Basin, with a focus on the region's cluster of elevated cancer mortalities. *Applied Geochemistry* 77: 178-183.
21. Liu JT, Cai WT, Cao YT, Cai YM, Bian C, Li YG, Chen YM (2018) Hydrochemical characteristics of groundwater and the origin in alluvial-proluvial fan of Qinhe River. *Environmental Science* 39(12): 5428-5439.
22. Rice EW, Baird RB, Eaton AD (2012) *Standard Methods for the Examination of Water and Wastewater* (23th Ed.). American Water Works Association, USA.
23. Shahid NM, Niazi K, Dumat C, Naidu R, Khalid S, Rahman MM, Bibi I (2018) A meta-analysis of the distribution, sources and health risks of arsenic-contaminated groundwater in Pakistan. *Environmental Pollution* 242(A):307-319.
24. WHO (World Health Organization) (2011) *Guidelines for drinking-water quality* (Fourth edition). The World Health Organization, Geneva, Switzerland, 1-564.
25. Taheri M, Mahmudy Gharraie MH, Mehrzad J, Afshari R, Datta S (2017) Hydrogeochemical and isotopic evaluation of arsenic contaminated waters in an argillic alteration zone. *Journal of Geochemical Exploration* 175:1-10.
26. Tang J, Lin NF, Bian JM, Liu WZ, Zhang ZL (1996) Environmental geochemistry of arsenic in the area of arsenic poisoning in Hetao Plain, Inner Mongolia. *Hydrogeology engineering geology* (1): 49-54.
27. Wang JH, Zhao LS, Wu YB (1998) Environmental geochemistry of arsenic in arsenism area of Shanyin and Yingxian, Shanxi Province. *Geoscience* 12 (2): 243-248.
28. Wen DG, Zhang FC, Zhang EY, Wang C, Han SB, Zheng Y (2013) Arsenic, fluoride and iodine in groundwater of China. *Journal of Geochemical Exploration* 135:1-21.
29. Xie XJ, Wang YX, Su CL, Li CX, Li MD (2012) Influence of irrigation practices on arsenic mobilization: Evidence from isotope composition and Cl/Br ratios in groundwater from Datong Basin, northern China. *Journal of Hydrology* 424-425:37-47.
30. Yang QC, Li ZJ., Ma HY, Wang LC, Martin JD (2016) Identification of the hydrogeochemical processes and assessment of groundwater quality using classic integrated geochemical methods in the Southeastern part of Ordos basin, China. *Environmental Pollution* 218: 879-888.
31. Zhang FC, Wen DG, Guo JJ, Zhang ER, Hao AB, Zhang YH (2010) Research progress and prospect of geological environment in main endemic areas of China. *Chinese geology in China* 37 (3): 551-562.
32. Zhang KX, Pan G, He W (2015) New division of tectonic-strata super region in China. *Earth Science* 40 (2), 206–233.

33. Zhang LK, Qin XQ, Tang JS, Liu W, Yang H (2017) Review of arsenic geochemical characteristics and its significance on arsenic pollution studies in karst groundwater, Southwest China. *Applied Geochemistry* 77: 80-88.
34. Zhu BQ, Yang XP, Rioual P, Qin XG, Liu ZT, Xiong HG, Yu JJ (2011) The Hydrogeochemistry of three watersheds (the Erlqis, Zhungarer and Yili) in northern Xinjiang, NW China. *Applied Geochemistry* 26 : 1535–1548.

Figures

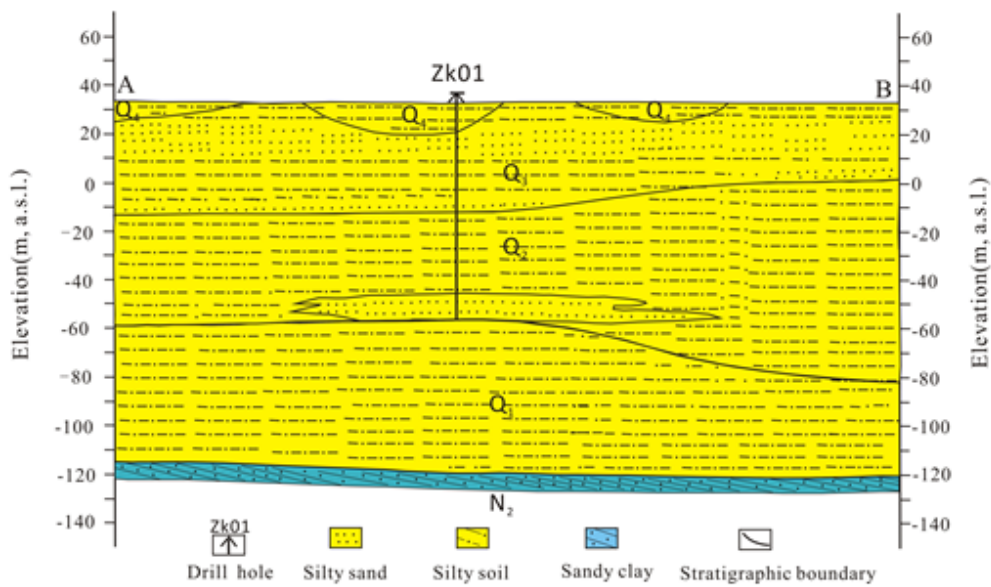
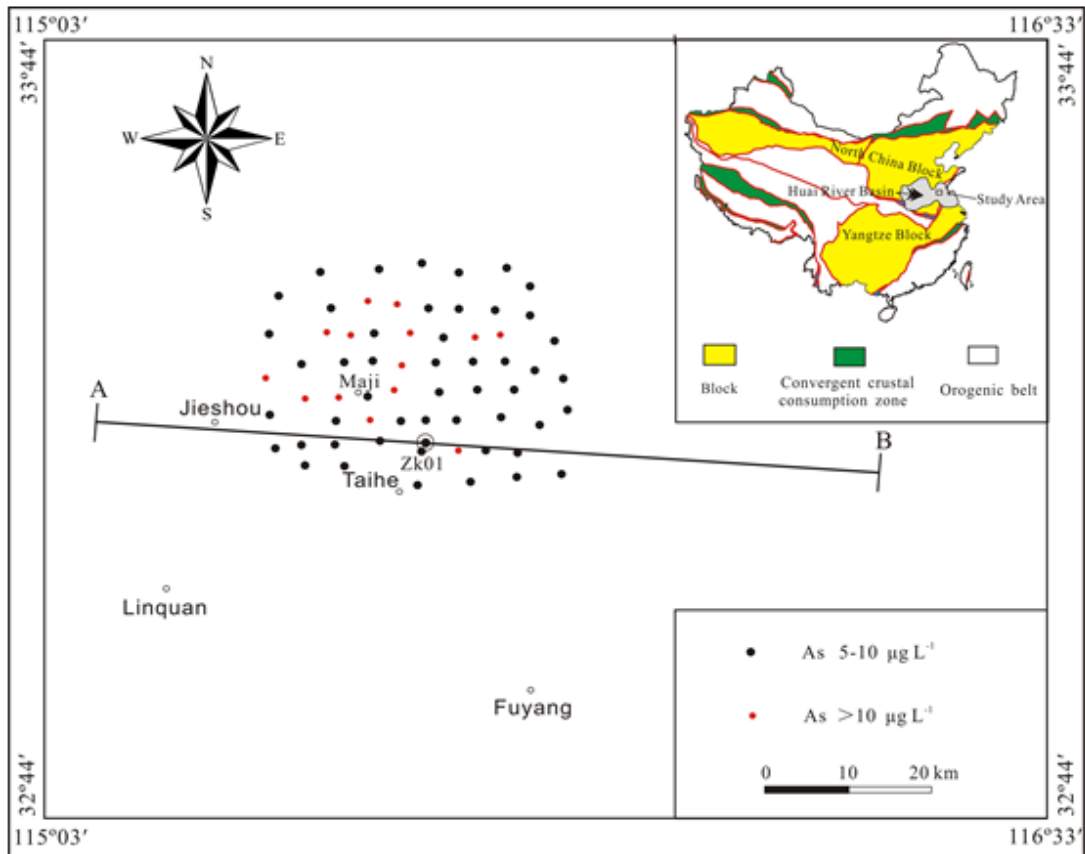


Figure 1

Geologic background, high-arsenic groundwater distribution and sampling points, and hydrogeological profile from Taihe, Anhui Province in Huaihe River Basin, China

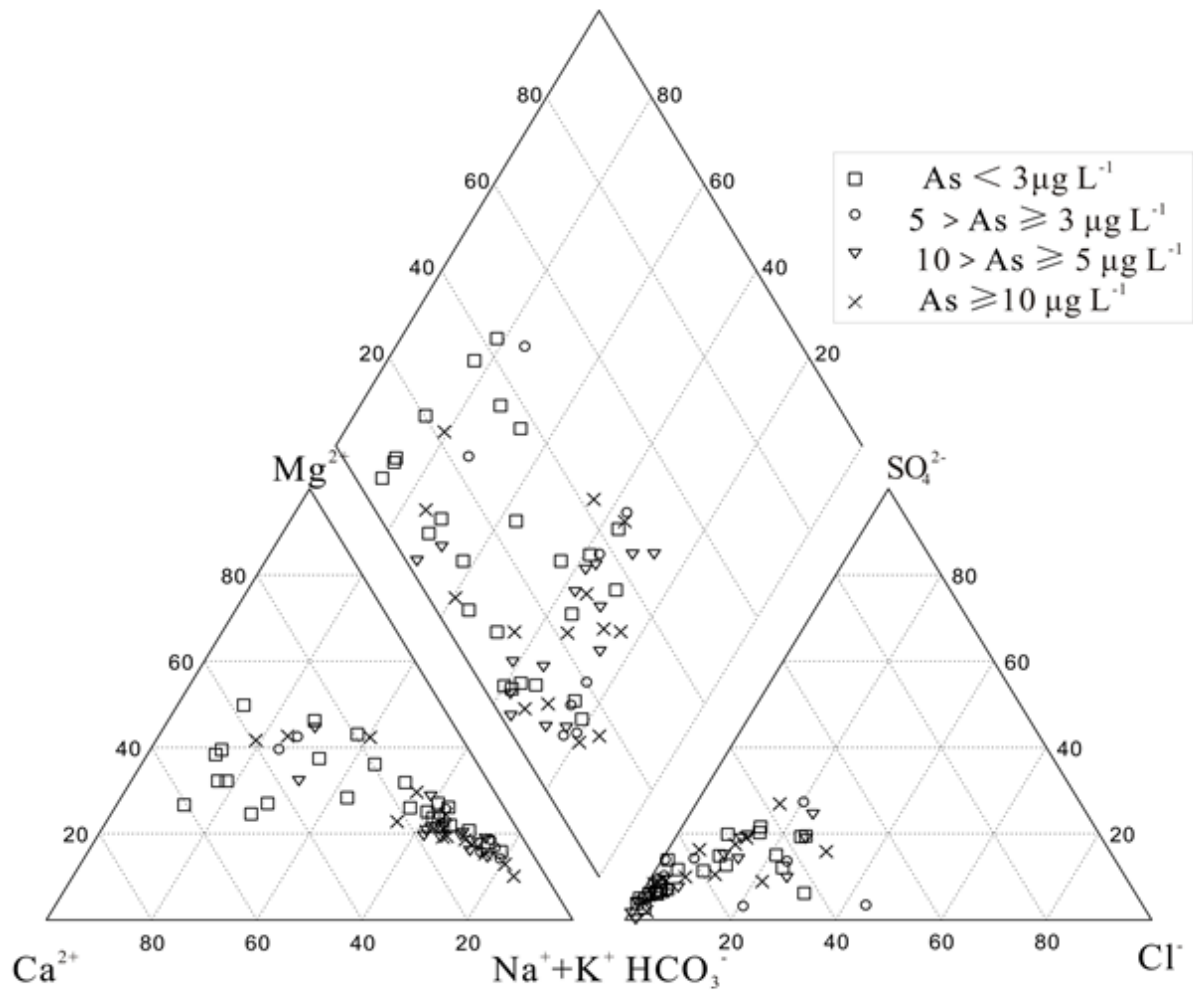


Figure 2

Piper diagram of the groundwater samples from Taihe, Anhui Province in Huaihe River Basin, China

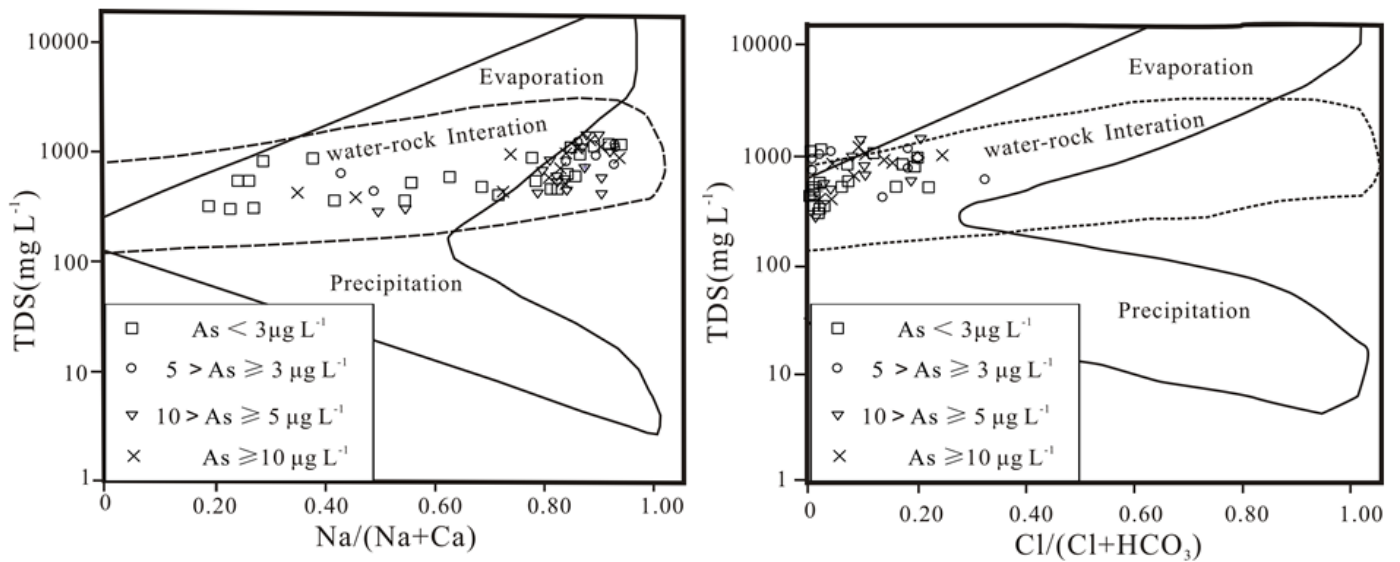


Figure 3

Gibbs diagram of hydrogeochemistry from Taihe, Anhui Province in Huaihe River Basin, China

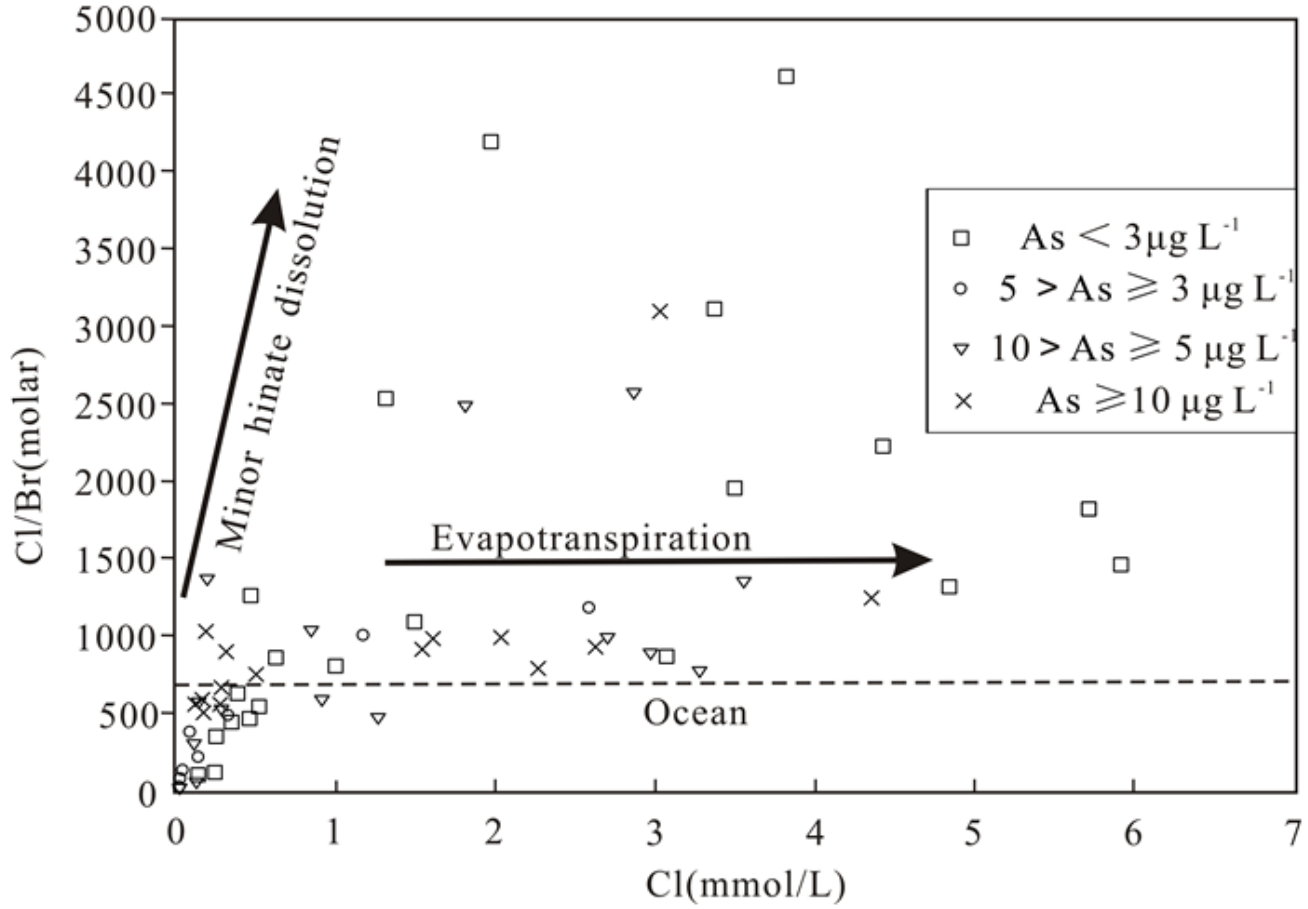


Figure 4

Correlation diagram of Cl/Br ratio and Cl in groundwater from Taihe, Anhui Province in Huaihe River Basin, China

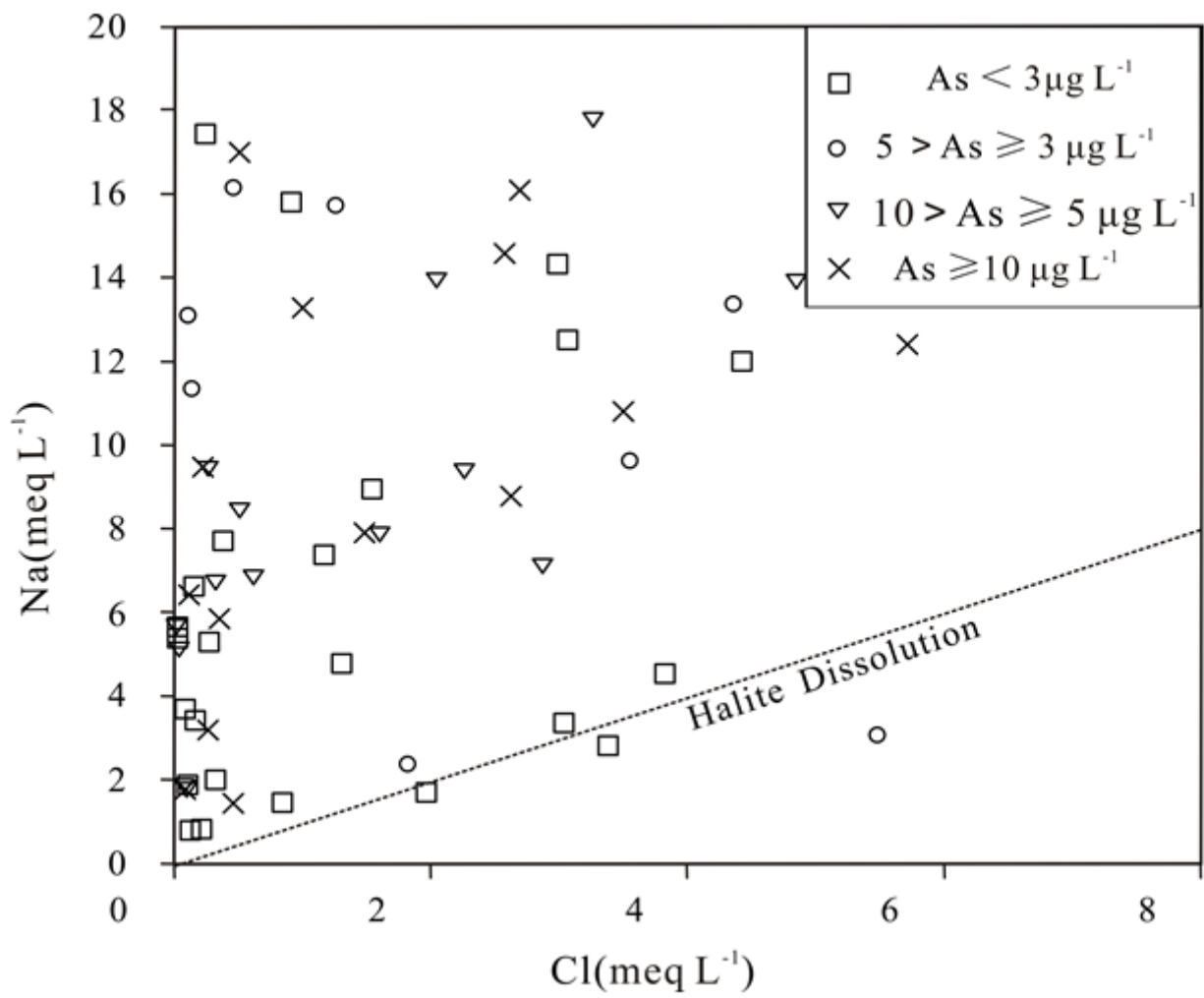


Figure 5

Diagram of Na-Cl in groundwater from Taihe, Anhui Province in Huaihe River Basin, China

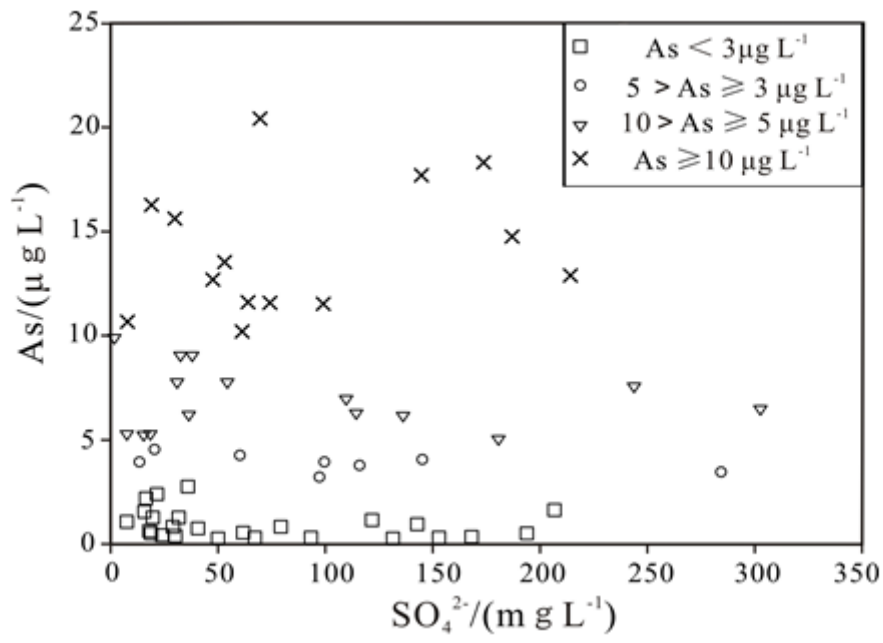


Figure 6

Correlation analysis of As-SO₄²⁻ in the groundwater from Taihe, Anhui Province in Huaihe River Basin